

# Type-II Colloidal Quantum Wells: CdSe/CdTe Core/Crown Heteronanoplatelets

Yusuf Kelestemur,<sup>†,‡</sup> Murat Olutas,<sup>†,‡,§</sup> Savas Delikanli,<sup>†</sup> Burak Guzel Turk,<sup>†,||</sup> Mehmet Zafer Akgul,<sup>†</sup> and Hilmi Volkan Demir<sup>\*,†,||</sup>

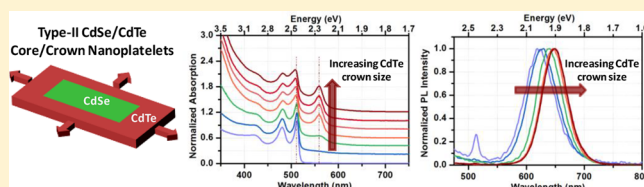
<sup>†</sup>Department of Electrical and Electronics Engineering, Department of Physics, UNAM—Institute of Materials Science and Nanotechnology, Bilkent University, Ankara 06800, Turkey

<sup>§</sup>Department of Physics, Abant Izzet Baysal University, Bolu 14280, Turkey

<sup>||</sup>Luminous! Center of Excellence for Semiconductor Lighting and Displays, School of Electrical and Electronic Engineering, School of Physical and Materials Sciences, Nanyang Technological University, Singapore 639798, Singapore

## S Supporting Information

**ABSTRACT:** Solution-processed quantum wells, also known as colloidal nanoplatelets (NPLs), are emerging as promising materials for colloidal optoelectronics. In this work, we report the synthesis and characterization of CdSe/CdTe core/crown NPLs exhibiting a Type-II electronic structure and Type-II specific optical properties. Here, based on a core-seeded approach, the CdSe/CdTe core/crown NPLs were synthesized with well-controlled CdTe crown coatings. Uniform and epitaxial growth of CdTe crown region was verified by using structural characterization techniques including transmission electron microscopy (TEM) with quantitative EDX analysis and X-ray diffraction (XRD). Also the optical properties were systematically studied in these Type-II NPLs that reveal strongly red-shifted photoluminescence (up to  $\sim 150$  nm) along with 2 orders of magnitude longer fluorescence lifetimes (up to 190 ns) compared to the Type-I NPLs owing to spatially indirect excitons at the Type-II interface between the CdSe core and the CdTe crown regions. Photoluminescence excitation spectroscopy confirms that this strongly red-shifted emission actually arises from the CdSe/CdTe NPLs. In addition, temperature-dependent time-resolved fluorescence spectroscopy was performed to reveal the temperature-dependent fluorescence decay kinetics of the Type-II NPLs exhibiting interesting behavior. Also, water-soluble Type-II NPLs were achieved via ligand exchange of the CdSe/CdTe core/crown NPLs by using 3-mercaptopropionic acid (MPA), which allows for enhanced charge extraction efficiency owing to their shorter chain length and enables high quality film formation by layer-by-layer (LBL) assembly. With all of these appealing properties, the CdSe/CdTe core/crown heterostructures having Type-II electronic structure presented here are highly promising for light-harvesting applications.



## INTRODUCTION

Semiconductor nanocrystals, which are also known as colloidal quantum dots, have been highly attractive materials for advanced optoelectronic device applications<sup>1–4</sup> with their size, shape, and composition tunable electronic structure and optical properties.<sup>5,6</sup> With the ease of facile colloidal synthesis of semiconductor nanocrystals, different kinds of core and core/shell architectures can be designed and synthesized with great control over their size distribution and shape uniformity.<sup>7–9</sup> Therefore, with the favorable selection of core and shell materials, electronic structure of semiconductor nanocrystals can be engineered to achieve either Type-I-like or Type-II-like electronic structure, which is highly critical for various applications.<sup>10–12</sup> For example, with the coating of higher band gap shell material, Type-I like electronic structure can be achieved where both electrons and holes are confined to the core. As a result of the confinement of the electron and hole inside the core region, higher oscillator strength and higher quantum yield can be obtained.<sup>13</sup> Recently, semiconductor nanocrystals having Type-I electronic structure have been

synthesized with almost near-unity quantum yield,<sup>14</sup> and this makes them highly promising candidates for the next generation light-emitting diodes<sup>15</sup> and lasing applications.<sup>16</sup>

In contrast to Type-I semiconductor nanocrystals, semiconductor nanocrystals having Type-II electronic structure, where there is a significantly reduced overlap between electron and hole wave functions, show different and interesting properties.<sup>12,17</sup> First, they exhibit strongly red-shifted emission originating from the radiative recombination of electron and hole across the core–shell interface, which would otherwise not be possible to achieve from either only core or only shell materials. Second, as a result of the separation of electron and hole wave functions, a reduced level of oscillator strength is observed with significantly increased radiative lifetime. In addition, thanks to the reduced oscillator strength, suppression of Auger recombination is also reported in Type-II semi-

Received: October 17, 2014

Revised: January 4, 2015

Published: January 5, 2015

conductor nanocrystals.<sup>11,18</sup> Therefore, with all of these attractive properties, Type-II nanocrystals are highly promising as light harvesting materials for photovoltaic and photo-conduction applications, where efficient removal of excited charges is highly desired.<sup>19</sup> However, when compared to the routinely synthesized highly efficient and stable Type-I semiconductor nanocrystals, Type-II semiconductor nanocrystals have suffered from the poor stability and impeded charge extraction. To date, different core/shell heterostructures including spherical forms,<sup>12,20</sup> rods,<sup>21,22</sup> tetrapods,<sup>23</sup> and barbells<sup>24,25</sup> having Type-II like band alignment have been synthesized and studied for the increased stability and enhanced charge extraction. Although higher quantum yield and stability have been reported for the spherical core/shell heterostructures having Type-II band alignment,<sup>26</sup> they suffer from the limited charge extraction since either electron or hole is always trapped inside the core of a spherical particle. On the other hand, while asymmetric core/shell heterostructures such as barbells and tetrapods enable more efficient charge extraction with respect to spherical ones, their inferior film formation limits the device performance.<sup>17</sup> Therefore, new architectures of colloidal semiconductor nanocrystals enabling efficient charge extraction and high quality film formation are welcomed for enhanced light harvesting purposes.

Recently, as a subclass of colloidal semiconductor nanocrystals, colloidal nanoplatelets (NPLs) have been introduced, which offer exciting properties owing to their quasi-1D confinement making them colloidal counterparts of quantum wells.<sup>27,28</sup> These NPLs exhibit extremely narrow emission bandwidth (<10 nm) with tunable peak emission via changing the thickness of the NPLs. In addition, assorted structures of NPLs having vertically grown shell region<sup>29</sup> and/or laterally grown crown region<sup>30,31</sup> can be synthesized with a precise control of the shell thickness and the crown width. With the formation of shell and crown region, core/shell and core/crown NPLs exhibit enhanced quantum yield and stability, which is indispensable for various advanced optoelectronic applications. For example, by using core/shell and core/crown NPLs having Type-I electronic structure, light-emitting diodes with a narrower emission bandwidth<sup>32</sup> and solution-processable laser with lower lasing threshold<sup>33</sup> have been demonstrated, respectively. However, NPLs having Type-II electronic structure have not previously been studied. Recently, during the review process of our work, the report by Pedetti et al. appeared to show the synthesis and characterization of CdSe/CdTe core/crown NPLs having Type-II electronic structure using a different cadmium precursor.<sup>34</sup>

Here, in an independent study, we report the synthesis of CdSe/CdTe core/crown NPLs having Type-II electronic structure with varying crown width by using core-seeded lateral shell growth approach. With the laterally grown CdTe crown region, atomically flat CdSe/CdTe core/crown NPLs are achieved, which is highly promising for efficiently removal of excited carriers. The epitaxial growth of CdTe crown layer is verified by using transmission electron microscopy (TEM) with quantitative EDAX analysis and X-ray diffraction (XRD). In these Type-II nanoplatelets, we systematically study the optical properties via tailoring the size of the CdTe crown layer. Strongly red-shifted photoluminescence (up to ~150 nm) is observed, which would not be possible to achieve from only 4 monolayer (ML) thick CdSe NPLs or CdTe NPLs. The fluorescence lifetimes of the Type-II NPLs are measured to be 2 orders of magnitude greater than those of the core-only Type-

I NPLs due to the presence of the spatially indirect excitons at the Type-II interface. Moreover, we extend the fluorescence time-resolved study and analyze temperature-dependent emission kinetics of CdSe/CdTe core/crown NPLs for a deeper understanding of their excitonic behavior. Although amplitude-averaged lifetimes of CdSe/CdTe core/crown NPLs slightly decrease with decreasing temperature, the fluorescence radiative lifetime components of CdSe/CdTe core/crown NPLs exhibit increasing behavior. Finally, we report an effective ligand exchange procedure to achieve water-soluble CdSe/CdTe core/crown NPLs, which may enable high quality film formation by using a layer-by-layer approach.

## ■ EXPERIMENTAL METHODS

**Chemicals.** Cadmium nitrate tetrahydrate ( $\text{Cd}(\text{NO}_3)_2 \cdot 4\text{H}_2\text{O}$ ) (99.999% trace metals basis), sodium myristate (>99%), technical grade 1-octadecene (ODE), selenium (Se) (99.999% trace metals basis), cadmium acetate dihydrate ( $\text{Cd}(\text{OAc})_2 \cdot 2\text{H}_2\text{O}$ ) (>98%), technical grade oleic acid (OA) (90%), technical grade trioctylphosphine (TOP) (90%), tellurium (Te) (99.997% trace metals basis), and 3-mercaptopropionic acid (>99%) were purchased from Sigma-Aldrich. Hexane, methanol, and ethanol were purchased from Merck Millipore.

**Preparation of Cadmium Myristate.** The preparation of cadmium myristate is followed by the recipe given in the literature.<sup>30</sup> Briefly, 1.23 g of cadmium nitrate tetrahydrate is dissolved in 40 mL of methanol, and 3.13 g of sodium myristate is dissolved in 250 mL of methanol. After complete dissolution, solutions are mixed and stirred strongly for around 1 h. Then, the solution is centrifuged and the precipitated part is dissolved in methanol. This washing step with methanol is performed at least three times for the removal of excess precursors. After that, the final precipitated part is kept under vacuum for about 24 h for drying.

**Synthesis of 4 ML Thick CdSe Nanoplatelets.** Four monolayer (ML) thick CdSe nanoplatelets (NPLs) are synthesized according to the recipe given in the literature.<sup>30</sup> For a typical synthesis, 170 mg of cadmium myristate, 12 mg of Se, and 15 mL of ODE are loaded into a three-neck flask. The solution is degassed at room temperature for half an hour to remove excess oxygen and volatile solvents. Then, the solution is heated to 240 °C under argon atmosphere. When the temperature reaches 195 °C, 80 mg of cadmium acetate dihydrate is introduced swiftly into the reaction. After the growth of CdSe NPLs at 240 °C for around 10 min, 0.5 mL of OA is injected and the temperature of the solution is decreased to room temperature. CdSe NPLs synthesized with this recipe exhibit peak emission at 513 nm, and other side products including NPLs having different thicknesses can be removed by size-selective precipitation. Finally, 4 ML thick CdSe NPLs are dissolved and stored in hexane.

**Preparation of Anisotropic Growth Mixture for CdTe Crown Region.** Anisotropic growth mixture is prepared with a slightly modified recipe, which is used for the growth of CdS crown region.<sup>30</sup> First, cadmium precursor is prepared. Briefly, 480 mg of cadmium acetate dihydrate, 340  $\mu\text{L}$  of OA, and 2 mL of ODE are loaded into a three-neck flask. The solution is heated to 150 °C under air with continuous stirring while also regularly sonicated. When a homogeneous gel having whitish color is formed, the solution is cooled down to room temperature. For the tellurium precursors, both Te-TOP (0.1 M) solution having an excess amount of TOP and Te-TOP-

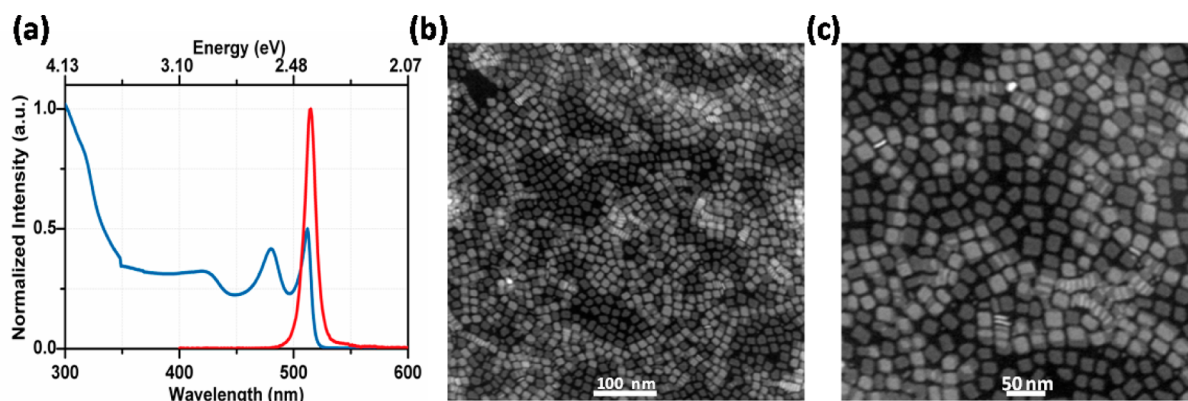


**Figure 1.** (a) Normalized absorption and photoluminescence spectra of 4 ML thick CdSe NPLs dissolved in hexane. High-angle annular dark-field transmission electron microscopy (HAADF-TEM) images of the 4 ML thick CdSe NPLs with a scale bar of (b) 100 nm and (c) 50 nm.

ODE (0.03 M) solution, which is achieved by the dilution of Te-TOP (1 M) solution with ODE, are prepared inside the glovebox.

**Synthesis of 4 ML Thick CdSe/CdTe Core/Crown Nanoplatelets.** CdSe/CdTe core/crown NPLs are synthesized using the core-seeded approach. For achieving a higher quantum yield, we have performed syntheses with slight modifications. In the first case, a certain amount of 4 ML thick CdSe NPLs dissolved in hexane and 5 mL of ODE were loaded into a three-neck flask. The solution was degassed at room temperature for 1 h for the complete removal of hexane. Then, the solution was further degassed at 100 °C for the removal of water and any other organic residuals. After that, the temperature was set to 240 °C under an argon atmosphere for the growth of the CdTe crown region. When the temperature reached 240 °C, anisotropic growth mixture including 2 mL of cadmium precursor and 3 mL of tellurium precursor having an excess amount of TOP was injected at the rate of 2.0 mL/h. Finally, with the addition of 0.5 mL of OA, the reaction was cooled down to room temperature. However, due to an excess amount of TOP, the resulting CdSe/CdTe core/crown NPLs exhibit lower quantum yield (<5%) with partial and/or nonuniform coating of CdTe crown region (Figure S1 in the Supporting Information). Recently, it has been demonstrated that while the presence of TOP in the reaction solution decreases the stability of CdSe core NPLs, the presence of carboxylates in the reaction solution preserves the stability of CdSe core NPLs.<sup>34</sup> Therefore, the amount of TOP in the Te precursor is critical in obtaining high quality CdSe/CdTe core/crown NPLs.

In the case of modified synthesis to achieve a higher quantum yield and uniform coating of CdTe crown region, Te-TOP-ODE (0.03 M) solution is used as a tellurium precursor and a calculated amount of cadmium precursor is added at the beginning of the reaction. For the synthesis, 2 mL of 4 ML thick CdSe NPLs dissolved in hexane (having optical density of 0.5 at 350 nm), 5 mL of ODE, 40  $\mu$ L of OA, and 0.39 mL of cadmium precursors were loaded into a three-neck flask. The solution was degassed at room temperature for 1 h for the complete removal of hexane. Then, the solution was further degassed at 100 °C for the removal of water and any other organic residuals. Subsequently, the temperature of the solution was set to 240 °C under argon atmosphere for the growth of CdTe crown region. When the temperature reached 240 °C, 1 mL of tellurium precursor (Te-TOP-ODE (0.03 M)) was injected at the rate of 8 mL/h and the synthesis was allowed to

react at 240 °C for 15 min (including injection) before cooling to room temperature. Finally, with the addition of 0.5 mL of OA, the reaction was cooled down to room temperature. By doing so, we achieved the highest quantum yield up to 40–50% with highly uniform coated CdTe crown region. In addition, depending on the desired size of CdTe crown region, the amount of cadmium and tellurium precursors could be changed. For the further characterization of CdSe/CdTe core/crown NPLs, they were cleaned with successive precipitation and dispersed in hexane.

**Ligand Exchange with 3-Mercaptopropionic Acid (MPA).** After the synthesis of CdSe/CdTe core/crown NPLs, ligand exchange is performed to achieve water-soluble colloidal nanoplatelets. For a typical ligand exchange procedure, 250  $\mu$ L of MPA is mixed with 15 mL of methanol and the mixture is shaken vigorously to homogeneously distribute MPA. Then, 30 mL of hexane is slowly added into the mixture. Afterward, NPLs dissolved in 2 mL of hexane are added dropwise while sonicating the mixture. After 30 min of sonication, the mixture is centrifuged at 4500 rpm until all of NPLs precipitate. The supernatant is discarded, and the precipitate is dissolved in deionized water. Then, the NPL solution is centrifuged at 2000 rpm for 5 min for the removal of the aggregated NPLs. The precipitate is discarded, and the resulting clear aqueous solution of NPLs is used for further studies.

## RESULTS AND DISCUSSION

In this study, 4 ML thick CdSe/CdTe core/crown NPLs having Type-II electronic structure are synthesized using the core-seeded approach. First, CdSe NPLs having 4 ML thickness are synthesized with a slightly modified recipe from the literature.<sup>30</sup> The absorption and photoluminescence spectra of 4 ML CdSe NPLs are given in Figure 1a. They have very sharp excitonic absorption peak at 513 nm corresponding to the electron/heavy-hole transition with a narrow emission line width having full width at half-maximum (fwhm) of  $\sim$ 8 nm. They exhibit a moderately high quantum yield (30–50%) when compared to bare CdSe core colloidal quantum dots. In addition, owing to the quantum-well-like structure of the NPLs, separation of heavy and light hole transitions is clearly observed in their absorption spectra. Moreover, depending on the synthesis parameters including the reaction temperature and time, the lateral dimensions of the NPLs can be tuned and either rectangular- or square-shaped NPLs can be achieved. As it can be seen from the transmission electron microscopy (TEM) images in Figures 1b and 1c, 4 ML CdSe NPLs, which are

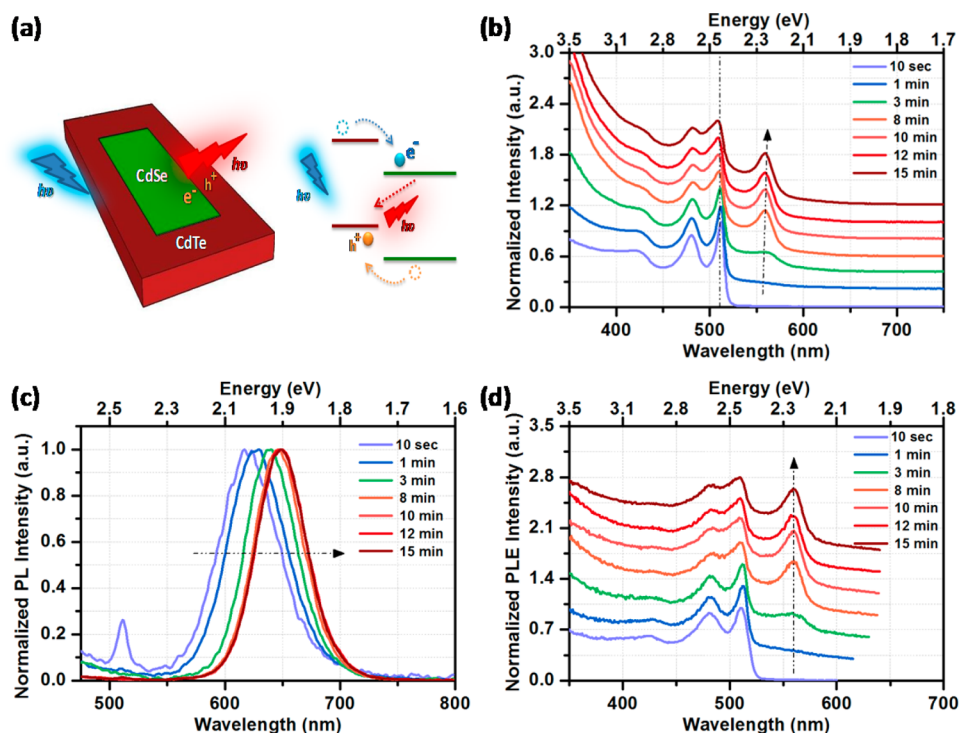


**Figure 2.** Optical characterization of 4 ML thick CdSe/CdTe core/crown NPLs having a higher quantum yield. (a) Schematic representation of carrier photogeneration in both CdSe-core and the CdTe-crown regions, transfer to core/crown interface, and subsequent radiative recombination resulting in Type-II emission. (b) Normalized absorption, (c) normalized photoluminescence (PL), and (d) normalized photoluminescence excitation (PLE) spectra of the CdSe/CdTe core/crown NPLs dissolved in hexane with varied crown size.

synthesized with the recipe given above, result in almost square shape with lateral dimensions of  $17.33 \text{ nm} \pm 1.51$  and  $13.31 \text{ nm} \pm 1.98 \text{ nm}$ .

By using the freshly synthesized CdSe NPLs as the seeds, CdSe/CdTe core/crown NPLs are synthesized with a continuous injection of crown precursors at higher temperatures, which is described in Experimental Methods in detail. Thanks to the anisotropic growth of cadmium acetate precursor, only lateral growth of CdTe is achieved. In addition, by simply changing the amount of injection, CdSe/CdTe core/crown NPLs with varied crown sizes are synthesized. Absorption spectra of CdSe/CdTe core/crown NPLs having a higher quantum yield are shown in Figure 2b. As it can be seen from the absorption spectra, the sharp excitonic transitions, which correspond to the electron/light-hole and electron/heavy-hole of CdSe, remain almost in the same spectral position during the growth of CdTe crown. These nonshifting excitonic features have also been observed for Type-I core/crown CdSe/CdS NPLs<sup>30,31</sup> and confirmed the growth of CdTe region only in the lateral direction. Otherwise, with the coating of CdTe region in the vertical direction, spectral shifting of the absorption peaks would be observed as a result of the delocalization of electron and hole wave functions across the whole structure. In addition, an absorption feature appearing within the spectral region of 550–560 nm emerges and becomes comparable to the electron/light-hole and electron/heavy-hole transitions of CdSe NPLs as the CdTe crown is grown larger. This red-shifted sharp absorption peak ( $\sim 556 \text{ nm}$ ) thus corresponds to the formation of excitons in the 4 ML thick CdTe crown layer,<sup>35</sup> and the intensity of this peak can be tuned by changing the size of the CdTe crown layer. Also, it was shown that higher concentration of OA results in formation of extended CdTe crown region and

enhances the absorption of crown region.<sup>34</sup> However, for the CdSe/CdTe core/crown NPLs synthesized by using an excess amount of TOP (Figure S1 in the Supporting Information), the excitonic peak corresponding to 4 ML thick CdTe crown layer could not be observed clearly, which can be attributed to the nonuniform and/or partial coating of CdTe crown region. Moreover, an absorption tail extending into the lower energy side of the absorption spectra is observed, and this can be attributed to the intermediate transitions at the core/crown interface owing to the Type-II band alignment.<sup>22,25</sup> Therefore, the growth of CdTe crown region occurs only in the lateral direction and both CdSe-core and CdTe-crown regions make contributions to the absorption. These features observed from the absorption spectra clearly indicate the formation of CdSe/CdTe core/crown NPLs having Type-II band alignment.

In addition to the absorption spectra of CdSe/CdTe core/crown NPLs having a higher quantum yield, the photoluminescence spectra (PL) are presented in Figure 2c. As it can be seen from the PL spectra, with a small amount of anisotropic growth mixture injection, the narrower emission of 4 ML thick CdSe NPLs is completely quenched and a broader emission that is strongly red-shifted as compared to the core-only NPLs is observed from the resulting CdSe/CdTe core/crown NPLs. Owing to the smaller Bohr radius of hole for CdTe ( $\sim 1.12 \text{ nm}$ ),<sup>34</sup> a very small layer coating of CdTe crown results in strongly red-shifted emission, which can be explained with the intermediate transition across the Type-II core/crown interface. Moreover, as the crown size is grown larger, the emission is continuously shifted from  $\sim 620$  to  $\sim 660 \text{ nm}$ , which can be attributed to the lateral confinement of CdTe crown region in addition to the vertical confinement. However, with the further injection of crown precursor, the emission peak remains almost in the same spectral position. Contrary to narrower emission

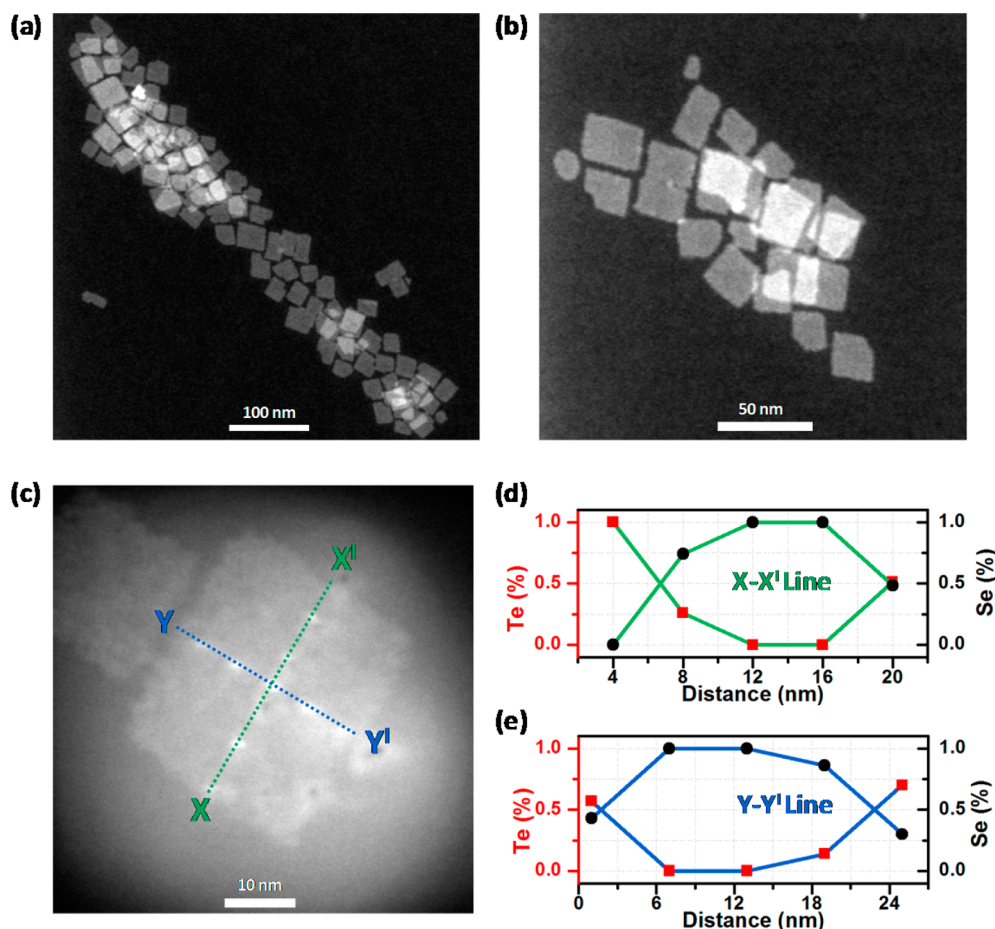


**Figure 3.** Structural characterization of 4 ML thick CdSe/CdTe core/crown NPLs having a higher quantum yield. High-angle annular dark-field transmission electron microscopy (HAADF-TEM) images of CdSe/CdTe core/crown NPLs with a scale bar of (a) 100 and (b) 50 nm. (c) HAADF-TEM image of a single CdSe/CdTe core/crown NPL, with blue (Y–Y<sup>I</sup>) and green lines (X–X<sup>I</sup>) showing the EDX probe position on CdSe/CdTe core/crown NPLs and (d, e) the line EDX analysis reporting the compositions of selenium and tellurium in the CdSe/CdTe core/crown NPLs, normalized to the total anionic composition.

line width of CdSe NPLs around 35 meV, the CdSe/CdTe core/crown NPLs exhibit broad emission line width, which is changing between 150 and 180 meV depending on the reaction time. While the CdSe/CdTe core/crown NPLs exhibit emission line width of  $\sim 180$  meV at the early stage of crown growth, the line width decreases down to  $\sim 150$  meV with the continuous injection of crown precursors. This behavior of CdSe/CdTe core/crown NPLs can be explained with the nonuniform coating of the CdTe crown region in the early stages of the crown growth. With the conformal coating of CdTe crown region at later stages, the line width starts to decrease during the reaction. Yet, the quantum yield and emission line width of CdSe/CdTe core/crown NPLs are strongly dependent on the reaction kinetics. For example, the excess amount of TOP used in the tellurium precursor promotes partial and/or nonuniform coating of CdTe crown region and results in lower quantum yield ( $<5\%$ ) with broader emission line width of  $\sim 200$  meV (Figure S1 in the Supporting Information). On the other hand, Te-TOP-ODE precursors having a lesser amount of TOP result in conformal coating of CdTe crown region with higher quantum yield (up to 40–50%) and narrower emission line width ( $\sim 150$  meV).

For a better understanding of the origin of strongly red-shifted emission, we also performed photoluminescence excitation (PLE) spectra measurements as shown in Figure

2d. As it can be seen from the PLE spectra of the CdSe/CdTe NPLs in the early stages of the crown growth, which are measured at the peak emission wavelength, the electron/light-hole and electron/heavy-hole transitions of CdSe NPLs are clearly observed. This indicates that this red-shifted emission originates from the excitons in the CdSe core. Moreover, the contribution from the CdTe crown layer starts to appear at the lower energy side with increasing size of the CdTe crown region. Then, by further increasing the size of CdTe crown region, it evolves into a sharp peak around 556 nm, which corresponds to the 4 ML thick CdTe crown region.<sup>35</sup> Finally, it can be concluded that the red-shifted emission originates from excitons formed in both the CdSe core region and the CdTe crown region, which is expected for Type-II materials.<sup>17,21</sup>

Moreover, by using transmission electron microscopy (TEM), quantitative EDX analysis, and X-ray diffraction (XRD), structural characterization of CdSe/CdTe core/crown NPLs was performed. HAADF-TEM images of CdSe/CdTe core/crown NPLs having a higher quantum yield are shown in Figures 3a and 3b. CdSe/CdTe core/crown NPLs exhibit increased lateral dimension  $28.81 \pm 4.30$  nm and  $22.86 \pm 3.51$  nm with respect to the CdSe core-only NPLs, which supports the growth of CdTe crown region. When compared to HAADF-TEM images of 4 ML thick CdSe NPLs, they exhibit rectangular shape with sharp boundaries, which is not observed

for CdSe/CdS core/crown NPLs.<sup>33</sup> Also, the size distribution of CdSe/CdTe core/crown NPLs is found to be increased.<sup>28</sup> In addition, we performed quantitative line EDX analysis for single CdSe/CdTe core/crown NPL confirming the formation core/crown architecture. While a higher amount of tellurium is observed for the outer parts or the crown region of the NPLs, a higher amount of selenium is measured for the inner part or the core region of the NPLs (Figure 3 d,e). Also, with the quantitative EDX analysis from the ensemble of CdSe/CdTe core/crown NPLs, coexistence of Se and Te is demonstrated (Figure S5 in the Supporting Information). In addition, the X-ray diffraction patterns of the CdSe core NPLs and CdSe/CdTe core/crown NPLs are given in Figure 4. As shown in

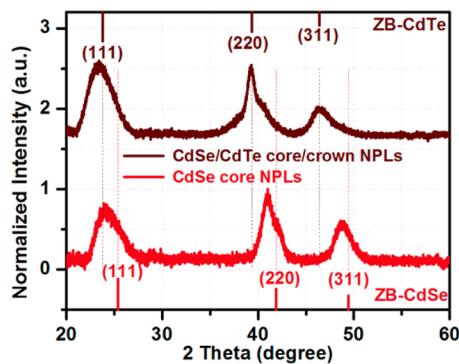


**Figure 4.** X-ray diffraction (XRD) pattern of 4 ML thick CdSe core NPLs and 4 ML thick CdSe/CdTe core/crown NPLs.

Figure 4, 4 ML thick CdSe core NPLs exhibit zinc-blende crystal structure with broader diffraction peaks. With the formation of thicker CdTe crown region, the diffraction peaks are shifted to the lower angles, which can be attributed to the formation of strain due to higher lattice mismatch between CdSe and CdTe. In addition, the well-resolved diffraction peaks of the CdSe/CdTe core/crown NPLs with respect to those of the CdSe core NPLs can be attributed to the increased size of NPLs and enhanced crystalline structure.

One of the most important features of semiconductor nanocrystals having Type-II electronic structure is their characteristic slow fluorescence emission decay kinetics. When compared to semiconductor nanocrystals with Type-I electronic structure, they exhibit longer radiative lifetime as a result of the spatial separation of electron and hole wave functions, where the electron (hole) wave function is localized in the CdSe-core (CdTe-crown) region. In order to verify this spatially distinct localization of the electron and hole wave functions and gain more physical insight into the Type-II electronic structure in the CdSe/CdTe core/crown NPLs, we conducted time-resolved fluorescence spectroscopy (TRF). TRF measurements were performed by using samples of NPLs in solution with low concentrations and under lower excitation intensities. Excitation pump source was a picosecond semiconductor laser diode at 3.31 eV. Fluorescence decay curves of CdSe/CdTe core/crown NPLs were measured at the emission peak wavelengths, which are presented in Figure 5. For a better understanding of emission kinetics, we compare the fluorescence decay curves of CdSe/CdTe core/crown NPLs having a higher quantum yield and lower quantum yield. These decay curves are analyzed by three-exponential decay functions resulting in reduced  $\chi^2$  about 1 with uniform residuals. As compared to 4 ML thick CdSe NPLs, with the growth of CdTe

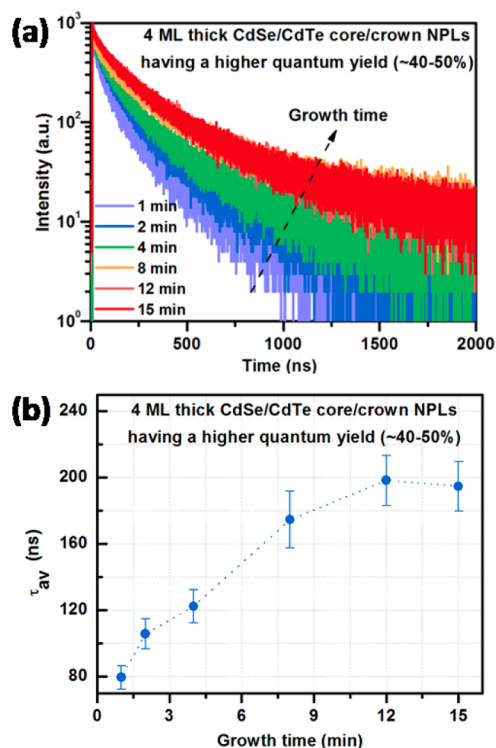


**Figure 5.** (a) Time-resolved fluorescence (TRF) decay curves of the CdSe/CdTe core/crown NPLs having a higher quantum yield with varied crown size and (b) the amplitude-averaged fluorescence lifetime.

crown region, longer amplitude-averaged fluorescence lifetimes are observed for both of the samples in the range of 130–190 ns depending on the crown size (Figure 5). Also, it was demonstrated that, with the synthesis of NPLs having a gradient core and/or an alloyed crown region, it is possible to tailor the average fluorescence lifetime of CdSe/CdTe NPLs.<sup>34</sup> Lifetime components and their fractional contributions are summarized in Figures S2 and S3 and Tables S1 and S2 in the Supporting Information. We find out three lifetime components for both of the samples: one on the order of 400–500 ns, another on the order of 100 ns, and a fast component on the order of 10 ns. The latter has very small fractional contribution to the emission kinetics (<5%), thus we attribute this fastest lifetime component to either partial coated NPLs or rapid nonradiative decay channel related to surface related traps in these NPLs. The observed two long fluorescence lifetime components are attributed to the radiative decay of the spatially indirect excitons at the Type-II interface. Previously, two similar decay channels were observed in CdTe/CdSe based colloidal quantum dots.<sup>36</sup> The origin of the coexistence is still under debate, however, these two long lifetime components clearly indicate that there are two distinct exciton states having Type-II properties with varying oscillator strength. A possible explanation might be the emissive mixed hole states (i.e., electron/light-hole and electron/heavy-hole) in these Type-II NPLs as supported by the broadening of the emission fwhm.

The trend of fluorescence lifetimes changing over the growth time of CdTe crown region is also summarized in Figure 5b. For example, the CdSe/CdTe core/crown NPLs having a higher quantum yield exhibit an amplitude-averaged fluorescence lifetime of  $\sim 100$  ns in the early stage of CdTe crown growth, and, with the increased size of CdTe crown region, the

amplitude-averaged fluorescence lifetime of CdSe/CdTe core/crown NPLs is continuously increased up to  $\sim 190$  ns. This can be explained with the strong delocalization of holes in the CdTe crown region, which results in the separation of electron and hole wave functions, leading to reduced oscillator strength and radiative decay rates. On the other hand, the CdSe/CdTe core/crown NPLs synthesized by using an excess amount of TOP in the tellurium precursor and having a lower quantum yield exhibit different behavior. The amplitude-averaged fluorescence lifetime is found to be  $\sim 120$  ns in the early stage of CdTe coating, and, with the extension of CdTe crown, the amplitude-averaged fluorescence lifetime of CdSe/CdTe core/crown NPLs is increased to  $\sim 160$  ns. However, with the further injection of CdTe crown precursors, although a strong separation of charge carriers in the CdSe/CdTe core/crown NPLs is achieved and an increase in the longer decay component is obtained, a decreased amplitude-averaged fluorescence lifetime ( $\sim 130$  ns) is observed. This can be explained with the formation of defect sites with the extended CdTe crown region possibly due to nonuniform coating and/or partial coating of CdSe NPLs, making the faster decay component dominant and decreasing the amplitude-averaged fluorescence lifetime of the CdSe/CdTe core/crown NPLs. These findings support the claim that the fast decay component observed for both of the CdSe/CdTe core/crown NPLs is originating from the formation of defect states and their contribution strongly depends on reaction kinetics and quality of the CdSe/CdTe core/crown NPLs.

Also, we extend the emission kinetics study employing temperature-dependent TRF for a better understanding of the excitonic behavior of the CdSe/CdTe core/crown NPLs with Type-II electronic structure. The CdSe/CdTe core/crown NPLs having the highest quantum yield were used for the temperature-dependent time-resolved fluorescence. For this study, a highly uniform film of CdSe/CdTe core/crown NPLs was prepared by spin-coating on a precleaned quartz substrate. Using closed-cycle He cryostat, the sample temperature was decreased from 297 to 20 K. While the fluorescence lifetime of the NPLs was measured from their spin-coated solid films to be  $\sim 190$  ns, the fluorescence lifetime of  $\sim 240$  ns was measured from the same NPLs in solution. This is partly attributed to the film effect since the NPLs are placed on the boundary of the quartz having a relatively high refractive index,<sup>37</sup> upon transferring them to the solid phase, which is also common in colloidal nanocrystals.<sup>38,39</sup> In addition, stacking of the NPLs in solid films can in part affect the decay kinetics.<sup>40</sup> As it can be seen from Figure 6, the amplitude-averaged fluorescence lifetime of the CdSe/CdTe core/crown NPLs are slightly decreased from  $\sim 190$  to  $\sim 170$  ns with decreasing temperature. Figure S4 and Table S3 in the Supporting Information show the fluorescence lifetime components as a function of the temperature, which were fitted using three exponential decay functions. Each fluorescence lifetime component is observed to grow longer with decreasing temperature. However, the decreased amplitude of the longest decay component ( $\tau_1$ ) led to decreased amplitude-averaged fluorescence lifetimes. The elongation of the radiative fluorescence lifetime components indicates that the electron and hole wave function separation must be increased as a result of the change of the coherence length of the excitons in the core/crown structure as the temperature is decreased. Therefore, excitons formed in the CdSe or CdTe part could be transferred to the interface more slowly. In addition, among the two emissive states ( $\tau_1$  and  $\tau_2$ ),

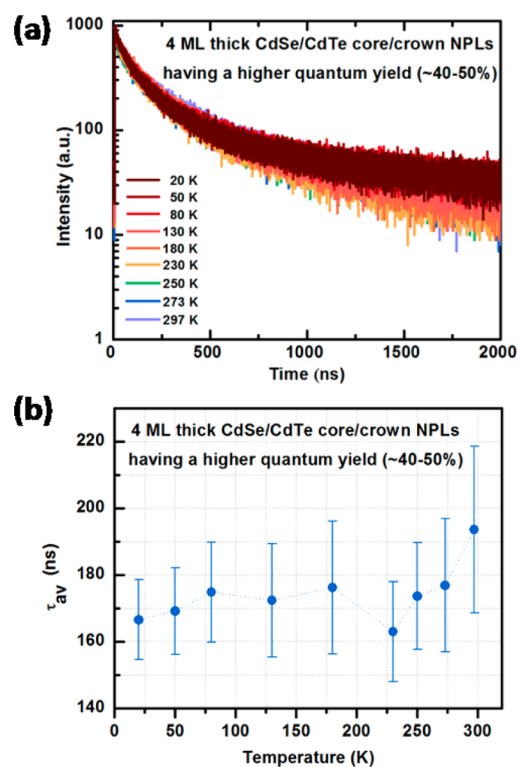


**Figure 6.** (a) Temperature-dependent time-resolved fluorescence (TRF) decay curves of the CdSe/CdTe core/crown NPLs having a higher quantum yield and (b) their amplitude-averaged fluorescence lifetime.

the amplitude of the  $\tau_2$  component increases with decreasing temperature and becomes dominant at lower temperatures. Increase in the fastest lifetime component might indicate slowing down of the nonradiative processes with decreasing temperatures. The complex decay kinetics should be further investigated, which will be our future work. When compared to Type-I NPLs, Type-II NPLs here exhibit interesting temperature dependency.

In addition to synthesis and characterization of the CdSe/CdTe core/crown NPLs, ligand exchange with 3-mercaptopropionic acid (MPA) was studied for achieving better properties. Compared to as-synthesized NPLs with long-chain ligands, NPLs with MPA ligands may offer great advantages including enhanced charge extraction thanks to their short-chain ligands and high quality film formation by using the layer-by-layer (LBL) assembly method, both of which might be highly crucial for a high performance device. First, as-synthesized 4 ML thick CdSe NPLs are used for the ligand exchange. The normalized absorption spectra of 4 ML thick CdSe NPLs dissolved in water and hexane are given in Figure 7a. After the ligand exchange with MPA, the sharp excitonic transitions corresponding to the electron/light-hole and electron/heavy-hole transitions are red-shifted by  $\sim 14$  and  $\sim 18$  nm, respectively. As a result of the coating of the surface of CdSe NPLs with a monolayer of sulfur atoms, electrons and holes are delocalized across the whole structure, which results in a decreased oscillator strength and a red-shifted absorption peak. In addition to the delocalization of electrons and holes, broadening of the electron/light-hole and electron/heavy-hole transition peaks are observed, which can be explained with the nonuniform surface coverage of ligands between NPLs. After that, ligand exchange procedure is performed for the CdSe/CdTe core/crown NPLs having a

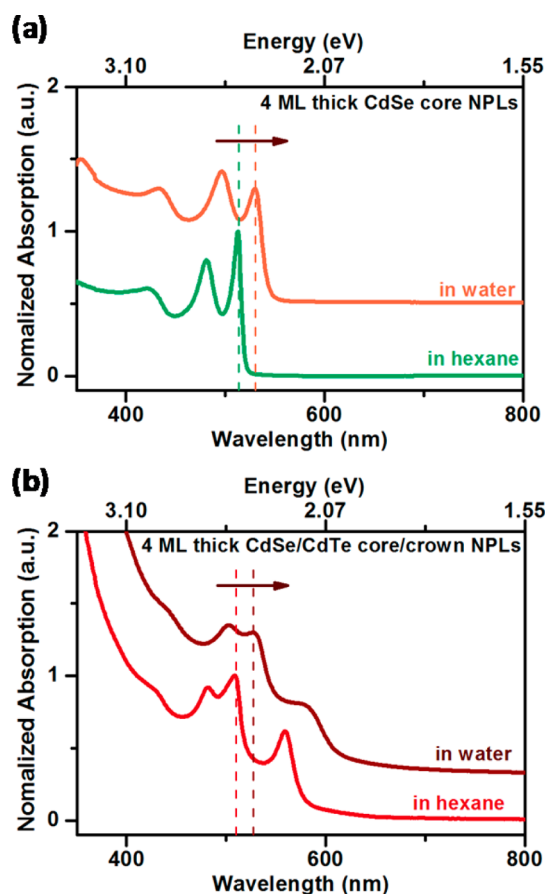


**Figure 7.** Normalized absorption spectra of (a) 4 ML thick CdSe core NPLs and (b) 4 ML thick CdSe/CdTe core/crown NPLs before and after the ligand exchange.

higher quantum yield. The normalized absorption spectra of 4 ML thick CdSe/CdTe core/crown NPLs dissolved in water and hexane are also given in Figure 7b. Similar to 4 ML thick CdSe NPLs, the same amount of shifting is observed for the electron/light-hole and the electron/heavy-hole transitions of the CdSe core region from the CdSe/CdTe core/crown NPLs. Moreover, similar to CdSe NPLs, the excitonic transition originating from CdTe crown region becomes clear after the ligand exchange with an approximately 30 nm red-shifted and broader peak. The lower intensity of the absorption tail extending into the lower energy side of spectra with a well-resolved excitonic transition of CdSe core region and CdTe crown region clearly indicates that, after the ligand exchange, the CdSe/CdTe core/crown NPLs are dissolved without any aggregation and/or stacking. However, these ligand-exchanged NPLs exhibit a very low quantum yield (<1%). Owing to the magic-sized thickness and very large surface area of NPLs, they are highly sensitive to surface modifications.

## CONCLUSION

In this study, we have demonstrated the synthesis and characterization of CdSe/CdTe core/crown NPLs having Type-II electronic structure. With a suitable crown shell precursor, atomically flat CdSe/CdTe core/crown NPLs are synthesized having well-controlled CdTe crown region widths and higher quantum yield up to 40–50%. By using TEM images with quantitative EDX analysis and XRD patterns, uniform and epitaxial growth of CdTe crown region is also

confirmed. With increasing width of the CdTe crown region, CdSe/CdTe core/crown NPLs exhibit strongly red-shifted photoluminescence originating from the intermediate transition across the core/crown interface. In addition, they exhibit significantly increased radiative lifetime characteristically for spatially distinct excitons formed at the Type-II interfaces. Finally, we performed ligand exchange with 3-mercaptopropionic acid (MPA) to reveal the potential of these NPLs as active media in advanced optoelectronic devices. With all of these promising properties, CdSe/CdTe core/crown NPLs hold great promise for next-generation light harvesting applications.

## ASSOCIATED CONTENT

### Supporting Information

Additional experimental figures of time-resolved fluorescence from CdSe/CdTe core/crown NPLs and tables of numerical analysis of time-resolved fluorescence measurements from CdSe/CdTe core/crown NPLs and EDX spectra of CdSe core NPLs and CdSe/CdTe core/crown NPLs. This material is available free of charge via the Internet at <http://pubs.acs.org>.

## AUTHOR INFORMATION

### Corresponding Author

\*E-mail: [volkan@bilkent.edu.tr](mailto:volkan@bilkent.edu.tr), [hvdemir@ntu.edu.sg](mailto:hvdemir@ntu.edu.sg).

### Author Contributions

‡Y.K. and M.O. contributed equally to this work.

### Notes

The authors declare no competing financial interest.

## ACKNOWLEDGMENTS

The authors would like to acknowledge the financial support from EU-FP7 Nanophotonics4Energy NoE, TUBITAK EEEAG 109E002, 109E004, 110E010, 110E217, NRF-RF-2009-09, NRF-CRP-6-2010-02, and A\*STAR of Singapore. H.V.D. acknowledges support from ESF-EURYI and TUBA-GEBIP. Y.K. acknowledges support from TUBITAK BIDEB.

## REFERENCES

- (1) Coe, S.; Woo, W. K.; Bawendi, M. G.; Bulović, V. Electroluminescence from Single Monolayers of Nanocrystals in Molecular Organic Devices. *Nature* **2002**, *420*, 800–803.
- (2) Klimov, V. I.; Mikhailovsky, A. A.; Xu, S.; Malko, A.; Hollingsworth, J. A.; Leatherdale, C. A.; Eisler, H.; Bawendi, M. G. Optical Gain and Stimulated Emission in Nanocrystal Quantum Dots. *Science* **2000**, *290*, 314–317.
- (3) Huynh, W. U.; Dittmer, J. J.; Alivisatos, A. P. Hybrid Nanorod-Polymer Solar Cells. *Science* **2002**, *295*, 2425–2427.
- (4) Mutlugun, E.; Soganci, I. M.; Demir, H. V. Photovoltaic Nanocrystal Scintillators Hybridized on Si Solar Cells for Enhanced Conversion Efficiency in UV. *Opt. Express* **2008**, *16*, 3537–3545.
- (5) Murray, C. B.; Norris, D. J.; Bawendi, M. G. Synthesis and Characterization of Nearly Monodisperse CdE (E = sulfur, selenium, tellurium) Semiconductor Nanocrystallites. *J. Am. Chem. Soc.* **1993**, *115*, 8706–8715.
- (6) Nizamoglu, S.; Mutlugun, E.; Özel, T.; Demir, H. V.; Sapra, S.; Gaponik, N.; Eychmüller, A. Dual-Color Emitting Quantum-Dot-Quantum-Well CdSe-ZnS Heteronanocrystals Hybridized on InGaN/GaN Light Emitting Diodes for High-Quality White Light Generation. *Appl. Phys. Lett.* **2008**, *92*, 113110.
- (7) Talapin, D. V.; Nelson, J. H.; Shevchenko, E. V.; Aloni, S.; Sadtler, B.; Alivisatos, A. P. Seeded Growth of Highly Luminescent CdSe/CdS Nanoheterostructures with Rod and Tetrapod Morphologies. *Nano Lett.* **2007**, *7*, 2951–2959.

- (8) Peng, X.; ScSchlamp, M. C.; Kadavanich, A. V.; Alivisatos, A. P. Epitaxial Growth of Highly Luminescent CdSe/CdS Core/Shell Nanocrystals with Photostability and Electronic Accessibility. *J. Am. Chem. Soc.* **1997**, *119*, 7019–7029.
- (9) Li, J. J.; Wang, Y. A.; Guo, W.; Keay, J. C.; Mishima, T. D.; Johnson, M. B.; Peng, X. Large-Scale Synthesis of Nearly Monodisperse CdSe/CdS Core/Shell Nanocrystals Using Air-Stable Reagents via Successive Ion Layer Adsorption and Reaction. *J. Am. Chem. Soc.* **2003**, *125*, 12567–12575.
- (10) Cihan, A. F.; Kelestemur, Y.; Guzelurk, B.; Yerli, O.; Kurum, U.; Yaglioglu, H. G.; Elmali, A.; Demir, H. V. Attractive versus Repulsive Excitonic Interactions of Colloidal Quantum Dots Control Blue- to Red-Shifting (and Non-shifting) Amplified Spontaneous Emission. *J. Phys. Chem. Lett.* **2013**, *4*, 4146–4152.
- (11) Klimov, V. I.; Ivanov, S. A.; Nanda, J.; Achermann, M.; Bezel, I.; McGuire, J. A.; Piryatinski, A. Single-Exciton Optical Gain in Semiconductor Nanocrystals. *Nature* **2007**, *447*, 441–446.
- (12) Kim, S.; Fisher, B.; Eisler, H. J.; Bawendi, M. Type-II Quantum Dots: CdTe/CdSe(Core/Shell) and CdSe/ZnTe(Core/Shell) Heterostructures. *J. Am. Chem. Soc.* **2003**, *125*, 11466–11467.
- (13) Dabbousi, B. O.; Rodriguez-Viejo, J.; Mikulec, F. V.; Heine, J. R.; Mattoussi, H.; Ober, R.; Jensen, K. F.; Bawendi, M. G. (CdSe)ZnS Core–Shell Quantum Dots: Synthesis and Characterization of a Size Series of Highly Luminescent Nanocrystallites. *J. Phys. Chem. B* **1997**, *101*, 9463–9475.
- (14) Greytak, A. B.; Allen, P. M.; Liu, W.; Zhao, J.; Young, E. R.; Popović, Z.; Walker, B. J.; Nocera, D. G.; Bawendi, M. G. Alternating Layer Addition Approach to CdSe/CdS core/shell Quantum Dots with Near-Unity Quantum Yield and High On-Time Fractions. *Chem. Sci.* **2012**, *3*, 2028–2034.
- (15) Mashford, B. S.; Stevenson, M.; Popovic, Z.; Hamilton, C.; Zhou, Z.; Breen, C.; Steckel, J.; Bulović, V.; Bawendi, M.; Coe-Sullivan, S.; Kazlas, P. T. High-Efficiency Quantum-Dot Light-Emitting Devices with Enhanced Charge Injection. *Nat. Photonics* **2013**, *7*, 407–412.
- (16) Dang, C.; Lee, J.; Breen, C.; Steckel, J. S.; Coe-Sullivan, S.; Nurmikko, A. Red, Green and Blue Lasing Enabled by Single-Exciton Gain in Colloidal Quantum Dot Films. *Nat. Nanotechnol.* **2012**, *7*, 335–339.
- (17) Lo, S. S.; Mirkovic, T.; Chuang, C. H.; Burda, C.; Scholes, G. D. Emergent Properties Resulting from Type-II Band Alignment in Semiconductor Nanoheterostructures. *Adv. Mater.* **2011**, *23*, 180–197.
- (18) Oron, D.; Kazes, M.; Banin, U. Multiexcitons in Type-II Colloidal Semiconductor Quantum Dots. *Phys. Rev. B* **2007**, *75*, 035330.
- (19) Zhu, H.; Song, N.; Lian, T. Wave Function Engineering for Ultrafast Charge Separation and Slow Charge Recombination in Type II Core/Shell Quantum Dots. *J. Am. Chem. Soc.* **2011**, *133*, 8762–8771.
- (20) Ivanov, S. A.; Piryatinski, A.; Nanda, J.; Tretiak, S.; Zavadil, K. R.; Wallace, W. O.; Werder, D.; Klimov, V. I. Type-II Core/Shell CdS/ZnSe Nanocrystals: Synthesis, Electronic Structures, and Spectroscopic Properties. *J. Am. Chem. Soc.* **2007**, *129*, 11708–11719.
- (21) Kumar, S.; Jones, M.; Lo, S. S.; Scholes, G. D. Nanorod Heterostructures Showing Photoinduced Charge Separation. *Small* **2007**, *3*, 1633–1639.
- (22) Saunders, A. E.; Koo, B.; Wang, X.; Shih, C. K.; Korgel, B. A. Structural Characterization and Temperature-Dependent Photoluminescence of Linear CdTe/CdSe/CdTe Heterostructure Nanorods. *ChemPhysChem* **2008**, *9*, 1158–1163.
- (23) Milliron, D. J.; Hughes, S. M.; Cui, Y.; Manna, L.; Li, J.; Wang, L. W.; Alivisatos, A. P. Colloidal Nanocrystal Heterostructures with Linear and Branched Topology. *Nature* **2004**, *430*, 190–195.
- (24) Halpert, J. E.; Porter, V. J.; Zimmer, J. P.; Bawendi, M. G. Synthesis of CdSe/CdTe Nanobells. *J. Am. Chem. Soc.* **2006**, *128*, 12590–12591.
- (25) Kirsanova, M.; Nemchinov, A.; Hewa-Kasakarage, N. N.; Schmall, N.; Zamkov, M. Synthesis of ZnSe/CdS/ZnSe Nanobells Showing Photoinduced Charge Separation. *Chem. Mater.* **2009**, *21*, 4305–4309.
- (26) Boldt, K.; Schwarz, K. N.; Kirkwood, N.; Smith, T. A.; Mulvaney, P. Electronic Structure Engineering in ZnSe/CdS Type-II Nanoparticles by Interface Alloying. *J. Phys. Chem. C* **2014**, *118*, 13276–13284.
- (27) Ithurria, S.; Dubertret, B. Quasi 2D Colloidal CdSe Platelets with Thicknesses Controlled at the Atomic Level. *J. Am. Chem. Soc.* **2008**, *130*, 16504–16505.
- (28) Ithurria, S.; Tessier, M. D.; Mahler, B.; Lobo, R. P. S. M.; Dubertret, B.; Efros, A. L. Colloidal Nanoplatelets with Two-Dimensional Electronic Structure. *Nat. Mater.* **2011**, *10*, 936–941.
- (29) Mahler, B.; Nadal, B.; Bouet, C.; Patriarche, G.; Dubertret, B. Core/Shell Colloidal Semiconductor Nanoplatelets. *J. Am. Chem. Soc.* **2012**, *134*, 18591–18598.
- (30) Tessier, M. D.; Spinicelli, P.; Dupont, D.; Patriarche, G.; Ithurria, S.; Dubertret, B. Efficient Exciton Concentrators Built from Colloidal Core/Crown CdSe/CdS Semiconductor Nanoplatelets. *Nano Lett.* **2014**, *14*, 207–213.
- (31) Prudnikau, A.; Chuvilin, A.; Artemyev, M. CdSe–CdS Nanoheteroplatelets with Efficient Photoexcitation of Central CdSe Region through Epitaxially Grown CdS Wings. *J. Am. Chem. Soc.* **2013**, *135*, 14476–14479.
- (32) Chen, Z.; Nadal, B.; Mahler, B.; Aubin, H.; Dubertret, B. Quasi-2D Colloidal Semiconductor Nanoplatelets for Narrow Electroluminescence. *Adv. Funct. Mater.* **2014**, *24*, 295–302.
- (33) Guzelurk, B.; Kelestemur, Y.; Olutas, M.; Delikanli, S.; Demir, H. V. Amplified Spontaneous Emission and Lasing in Colloidal Nanoplatelets. *ACS Nano* **2014**, *8*, 6599–6605.
- (34) Pedetti, S.; Ithurria, S.; Heuclin, H.; Patriarche, G.; Dubertret, B. Type-II CdSe/CdTe Core/Crown Semiconductor Nanoplatelets. *J. Am. Chem. Soc.* **2014**, *136*, 16430–16438.
- (35) Pedetti, S.; Nadal, B.; Lhuillier, E.; Mahler, B.; Bouet, C.; Abecassis, B.; Xu, X.; Dubertret, B. Optimized Synthesis of CdTe Nanoplatelets and Photoresponse of CdTe Nanoplatelets Films. *Chem. Mater.* **2013**, *25*, 2455–2462.
- (36) de Mello Donegá, C. Formation of Nanoscale Spatially Indirect Excitons: Evolution of The Type-II Optical Character of CdTe/CdSe Heteronanocrystals. *Phys. Rev. B* **2010**, *81*, 165303.
- (37) Novotny, L.; Hecht, B. *Principles of Nano-Optics*; Cambridge University Press: 2012.
- (38) Guzelurk, B.; Martinez, P. L. H.; Zhang, Q.; Xiong, Q.; Sun, H.; Sun, X. W.; Govorov, A. O.; Demir, H. V. Excitonics of Semiconductor Quantum Dots and Wires for Lighting and Displays. *Laser Photonics Rev.* **2014**, *8*, 73–93.
- (39) Yeltik, A.; Guzelurk, B.; Hernandez-Martinez, P.; Govorov, A. O.; Demir, H. V. Phonon-Assisted Exciton Transfer into Silicon Using Nanoemitters: The Role of Phonons and Temperature Effects in Förster Resonance Energy Transfer. *ACS Nano* **2013**, *7*, 10492–10501.
- (40) Guzelurk, B.; Erdem, O.; Olutas, M.; Kelestemur, Y.; Demir, H. V. Stacking in Colloidal Nanoplatelets: Tuning Excitonic Properties. *ACS Nano* **2014**, *8*, 12524–12533.